Rho-dependent Termination within the *trp t′* Terminator. II. Effects of Kinetic Competition and Rho Processivity†

Anne Q. Zhu‡ and Peter H. von Hippel*

Institute of Molecular Biology and Department of Chemistry, University of Oregon, Eugene, Oregon 97403-1229

Received November 26, 1997; Revised Manuscript Received May 6, 1998

ABSTRACT: Continuing our quantitative analysis of rho-dependent termination at the *trp t′* terminator, we here present evidence that the position of rho-dependent terminators along the template is strongly regulated by the secondary structure of the nascent RNA transcript, and that the prerequisite for establishing an effective kinetic competition between elongation and rho-dependent RNA release at a particular termination position is an upstream rho hexamer properly bound to a rho loading site on the nascent transcript. As a consequence kinetic competition regulates termination efficiency at individual positions downstream of the rho loading site, but does not control the *position* of the termination zone. Conditions that favor the formation of stable secondary structure on the RNA shift the initial rho-dependent termination position downstream. These results are consistent with a model that states that the rho protein requires ∼70−80 nucleotide residues of unstructured RNA to load onto the transcript and cause termination, and that stable RNA secondary structures are effectively "looped out" to avoid interaction with rho, meaning that more RNA must be synthesized before rho-dependent termination can begin. Thus, although the rate of transcript elongation is important in determining termination efficiency at specific template positions, the process of loading of the rho hexamer onto the nascent transcript plays an overriding role in determining the template positions of rho-dependent terminators. We also show that at high salt concentrations, which have virtually no effect on the rate of transcript elongation, rho-dependent transcript termination is more directly dependent on the efficiency of rho loading, since the processivity of translocation of rho along the nascent transcript to "catch up with" the polymerase is much more limited under these conditions. A quantitative model for rho-dependent transcript termination is developed to account for all these interacting effects of rho on the efficiency of RNA release from actively transcribing elongation complexes.

In the preceding paper (*1*) we showed that transcript termination under conditions of high overall rho-dependent termination efficiency can begin within the previously defined rho "loading site" of the *trp t′* terminator even before the putatively essential *rut*B sequence has been transcribed. We also showed that the presence of RNA secondary structure within the actual site of rho loading shifts the beginning of the rho-dependent termination zone downstream along the template that contains a *trp t′* terminator, and that this effect can be relieved by destabilizing the secondary structure of the RNA by replacing guanosine residues in the transcript with inosine residues. This replacement resulted in no changes in the rate of synthesis by the transcription complex at the new termination sites, demonstrating that the presence of elements of RNA secondary structure within the actual rho loading site is primarily responsible for establishing the upstream limit of the zone within which rho-dependent termination can occur, and that the template position of this limit is independent of the rate of transcript elongation.

Here we extend these observations by testing in detail the effects of the RNA secondary structure within the actual rho loading zone on: (i) the position of the upstream edge of the termination zone along the template; and (ii) the efficiency of rho-dependent termination at individual template positions within the termination zone. We show that decreasing the rate of transcript elongation does not change the position of the termination zone along the template, but does increase termination efficiency at individual termination positions. We further show that high concentrations of K^+ or Mg^{2+} ions, which serve both to destabilize the binding of rho to the nascent RNA and to induce additional secondary structure in the transcript, do not increase the rate of transcript elongation. However, these increased cation concentrations do shift the termination zone downstream and decrease termination efficiency, and these salt concentration effects are only partially compensated by major decreases in the elongation rate of the transcription complex. Finally the results presented in this paper and the companion paper (*1*), together with the structural and mechanistic findings of others, are used to formulate a quantitative model for the efficiency of rho-dependent transcript termination as a function of template position, rho loading, and translocation processivity, and the kinetic competition between the rates of rho-dependent termination and transcript elongation.

† This research was supported in part by USPHS Research Grants GM-15792 and GM-29158 (to P.H.v.H.) and was submitted (by A.Q.Z.) to the Graduate School of the University of Oregon in partial fulfillment of the requirements for the Ph.D. degree in Chemistry. P.H.v.H. is an American Cancer Society Research Professor of Chemistry.

* Corresponding author. E-mail: petevh@molbio.uoregon.edu.

‡ Present address: Howard Hughes Medical Institute, University of Chicago, Box MC1028 N125, Chicago, IL 60637.

S0006-2960(97)02912-7 CCC: $15.00
Published on Web 07/24/1998

MATERIALS AND METHODS

All the Materials and Methods used in this study are described in the preceding paper (*1*), except as follows.

Measurement of Elongation Rates. Elongation complexes paused at position +25[1] were prepared as described in Materials and Methods of the preceding paper (*1*). Samples were then adjusted to the desired KCl and $MgCl_2$ concentrations, divided into individual transcription reactions, and held at 0 °C. Individual reaction tubes were preincubated at room temperature for 20 s prior to use, and transcription was started at 0 time by adding the desired concentrations of NTP substrates, together with 10 μg/mL of rifampicin. Reactions were quenched at various times and subjected to gel electrophoresis and ImageQuant analysis (see Materials and Methods, and Figure 3A of the preceding paper), and the amount of runoff transcript in each reaction lane of the gel was determined. From these results the time ($t_{0.5}$) at which one-half of the population of complexes had reached the end of the template was calculated for each reaction. The average elongation rate, *R*, in nts/s,[2] was then calculated as

$$R = (N - 25)/t_{0.5} \quad (1)$$

where *N* is the length of the runoff transcript in nucleotide residues (nts) and 25 nts is the length of the transcript within the initially stalled elongation complex.

We have also fit the data representing the accumulation of runoff transcripts as a function of the elongation time with a mathematical description of the chemical kinetics of elongation presented by Capellos and Bielski (*2*). We found that the elongation reaction that converts the initial +25 complexes to runoff transcript is dominated by a few relatively slow steps that can be visualized as transient bands on the radioactive gels of the elongation reactions. Average elongation rates deduced from such a mathematical description of the entire elongation process were indistinguishable from those determined using eq 1 above (data not shown).

RESULTS

The Position of the Termination Zone Within Rho-Dependent Terminators is Not Controlled by Kinetic Competition. Kinetic competition between the rates of rho function (as manifested by ATPase activity) and transcript elongation has been shown to modulate rho-dependent termination efficiency at the *tR1* terminator of phage λ (*3*). However, these results did not reveal whether or how this kinetic competition might affect the position of the rho-dependent termination zone. In the preceding paper (*1*) we showed that the proximal shift of the termination zone on the NInt′ template that resulted from the incorporation of rI residues into the transcript in the place of rG residues did not result in any significant change in the kinetics of transcript elongation at the new termination positions. To further test for possible effects of kinetic competition on the position of the zone of rho-dependent termination within the

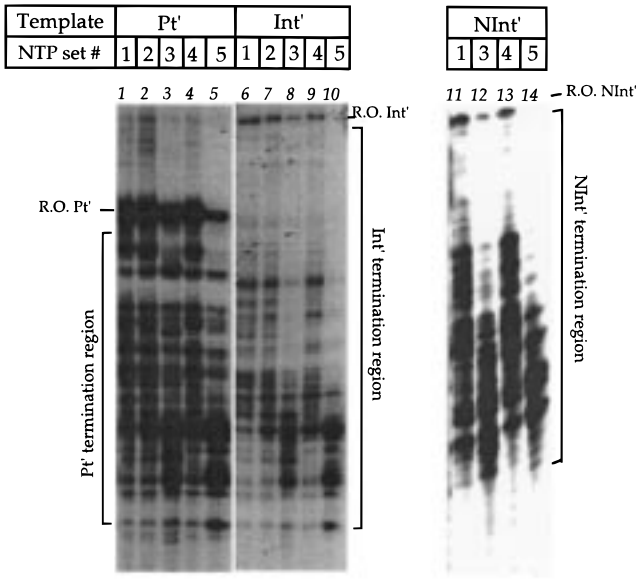

FIGURE 1: The template zone in which rho-dependent termination occurs is not defined by kinetic competition. Rho-dependent termination reactions were performed at different NTP substrate concentrations. Radioactive bands that correspond to runoff transcripts for different templates are marked in the margins. Transcription reactions were carried out under standard reaction conditions (20 mM Tris-HCl (pH 7.9), 50 mM KCl, 5 mM $MgCl_2$, 1 mM β-ME) in the presence of 5 nM DNA template, 5 nM RNA polymerase, and 20 nM rho hexamer (as described in Materials and Methods of ref *1*), except NTP concentrations were as follows: set 1, 1 mM concentrations of each NTP; set 2, 100 μM concentrations of each NTP; set 3, 10 μM concentrations each NTP; set 4, 1 mM ATP and 100 μM concentrations of each of the other NTPs; set 5, 1 mM ATP and 10 μM concentrations of each of the other NTPs.

trp t′ terminator, we have mapped the rho-dependent termination zone on all three templates used in this study (see Figure 1 of the preceding paper for the designations and construction of these templates) at five different sets of NTP concentrations. NTP concentrations well below the apparent K_m values for the elongation reaction were used for the experiments at low substrate levels, thus making the binding of the next required NTP the rate-limiting step for elongation (*4, 5*).

These experiments were setup as follows. Substrate set *1* contained a final concentration of 1 mM of each NTP; set *2* contained 100 μM concentrations of each NTP; set *3* contained 10 μM concentrations of each NTP; set *4* contained 1 mM ATP and 100 μM concentrations of each of the other NTPs; and set *5* contained 1 mM ATP and 10 μM concentrations of each of the other NTPs. It should be noted that the ATP concentration in sets *4* and *5* was maintained at 1 mM to ensure that the rho function, which is dependent on its RNA-dependent ATPase activity, was not perturbed by any NTP concentration dependent slowing of the transcript elongation rate.

We found that the overall efficiency of rho-dependent termination increases with decreasing concentrations of NTPs on all templates, as shown in Figure 1, lanes 1−5, for template Pt′, lanes 6−10 for template Int′, and lanes 11−14 for template NInt′. We have measured the average elongation rate (see Materials and Methods) on template NInt′ at the different substrate concentrations used, and the results are listed in Table 1. We show that a 10-fold decrease in

[1] Template positions are designated by the length of the corresponding transcript. Thus +1 is the position of chain initiation at the promoter and +25 is the template position at which the 3′ terminus of the nascent transcript is located for an RNA transcript that is 25 nts in length.

[2] Abbreviations: nt(s), nucleotide residue(s); bp(s), base pair(s); NTP(s), nucleoside-5′-triphosphate(s).

Table 1: Average RNA Polymerase Elongation Rates under Different Reaction Conditions[a]

reaction conditions			
[KCL] (mM)	[Mg^{2+}] (mM)	[NTP] (mM)	average elongation rates[a]
		1	13.03 ± 2.38
50	5	0.1	3.9 ± 0.2
		0.01	1.3 ± 0.3
200	5	1	13.3 ± 2.8
50	20	1	8.7 ± 1.1
50	5	1 (with ITP)	5.7 ± 0.2

[a] Elongation rates are in units of nt s^{-1}. All measurements are performed at room temperature with the NInt′ template, as described in Materials and Methods. Each measurement was repeated at least three times.

substrate concentration (from 1 mM to 100 μM NTPs) slows the average rate of transcript elongation about 3-fold, while a further 10-fold decrease (from 100 μM to 10 μM NTPs) slows elongation by another factor of 3.

These results are consistent with the kinetic competition model in that, as expected, the termination function of rho appears to compete with the rate of transcript elongation in modulating termination efficiency. However, we also found that no rho-dependent termination is seen at any position upstream of position +97 on templates Pt′ and Int′, or of position +123 on template NInt′, even when the concentration of substrate NTPs is decreased 100-fold to produce an ~10-fold decrease in the rate of transcript elongation. These observations demonstrate that while the termination efficiency of rho is modulated by kinetic competition between rho and RNA polymerase at positions *within* the rho-dependent terminator, the actual template *position* of the termination zone along the template appears to be entirely dependent on a rho loading event that is not affected by changes in the rate of transcript elongation.

Effects of Salt Concentrations on Elongation and Rho-Dependent Termination. High concentrations of monovalent and divalent cations have been shown to decrease the efficiency of rho-dependent termination (*6*). Since increased salt concentrations also decrease the stability of rho−RNA interactions and promote secondary structure formation in RNA (*7, 8*), we have investigated the effects of increasing concentrations of K^+ and Mg^{2+} on rho-dependent termination in more detail.

(i) Effects of Increased KCl Concentrations. The effects of increasing concentrations of KCl[3] were examined with all three templates, and the results show that the overall efficiency of rho-dependent termination decreases with an increase in monovalent cation concentration, with RNA release being reduced to less than 10% of its low salt concentration level at 200 mM KCl. This effect is demonstrated in the form of gel patterns for template NInt′ in Figure 2A, while the dependence of the overall termination efficiency, TE_ρ (as defined in ref *1*), on the concentration of KCl is shown in Figure 2B.

More can be learned about these effects by careful examination of the rho-dependent RNA release patterns at the different salt concentrations. Figure 2C shows a typical release pattern measured on template NInt′ under our standard reaction conditions in 50 mM KCl (dark solid line) and 150 mM KCl (faint solid line). Clearly rho-dependent termination is decreased at most termination positions at the higher salt concentration, but this effect is most severe at early termination sites, resulting in an apparent downstream shift of the major termination zone. This effect is more evident when termination efficiencies at higher KCl concentrations are expressed as fractions of those measured in 50 mM KCl for the same template positions. Such relative values of Te_ρ are plotted as a function of template position in Figure 2D.

Two sets of patterns are shown in Figure 2D, with the solid lines corresponding to template Pt′ and the dotted lines to template NInt′. The pattern obtained with the Pt′ template shows more fine structure than that measured with template NInt′, since the termination zone along Pt′ was divided into more grid boxes and thus the rho-dependent termination pattern along template Pt′ is more clearly resolved. The patterns numbered 1−3 in each group represent the relative (to 50 mM KCl conditions) values of Te_ρ for reactions containing 100, 150, and 200 mM KCl, respectively, for the two templates. Clearly the two groups of curves run roughly parallel to one another at most positions and display roughly hyperbolic shapes. This means that rho-dependent transcript termination for both templates is most severely inhibited at the most proximal positions at higher salt concentrations, as expected from our qualitative observation that the apparent termination zone is shifted downstream at higher KCl concentrations (see Figure 2A).

Table 1 shows that the average transcript elongation rate is essentially the same in solutions containing either 50 or 200 mM KCl, although the value of TE_ρ over this KCl concentration range decreases from ~1.0 to ~0.1 (Figure 2B). The former finding is consistent with the comparable measurements of others (*9*) on the effects of salt concentrations on the rates of transcription elongation. We reasoned that if rho-dependent termination at the proximal template positions had been selectively decreased by a decreased rate of rho function at higher salt concentrations, then slowing elongation by decreasing the concentration of NTP substrates below K_m might compensate and restore rho-dependent termination at proximal positions within the terminator. To test this hypothesis, values of Te_ρ were measured at individual template positions on the NInt′ template at 150 mM KCl concentrations under the five sets of substrate concentrations defined above.

The dotted line in Figure 2C represents the pattern of rho-dependent RNA release on the NInt′ template in 150 mM KCl under NTP concentration condition set 3 (above). It is apparent that even though a slower rate of transcript elongation does increase Te_ρ at corresponding template positions (compare the dotted line with the faint solid line), the proximal termination sites are largely not reactivated (compare the dotted line with the dark solid line). Results at other substrate concentration conditions are qualitatively the same (data not shown). Thus shifting the balance of the kinetic competition between rho-dependent RNA release and elongation toward rho function (by an additional factor of ~3 as estimated from Table 1) does not restore the proximal peaks of the 50 mM KCl rho-dependent RNA release pattern, even though such compensating effects are seen at the more distal template positions.

[3] Essentially identical results were obtained if KOAc was used instead of KCl.

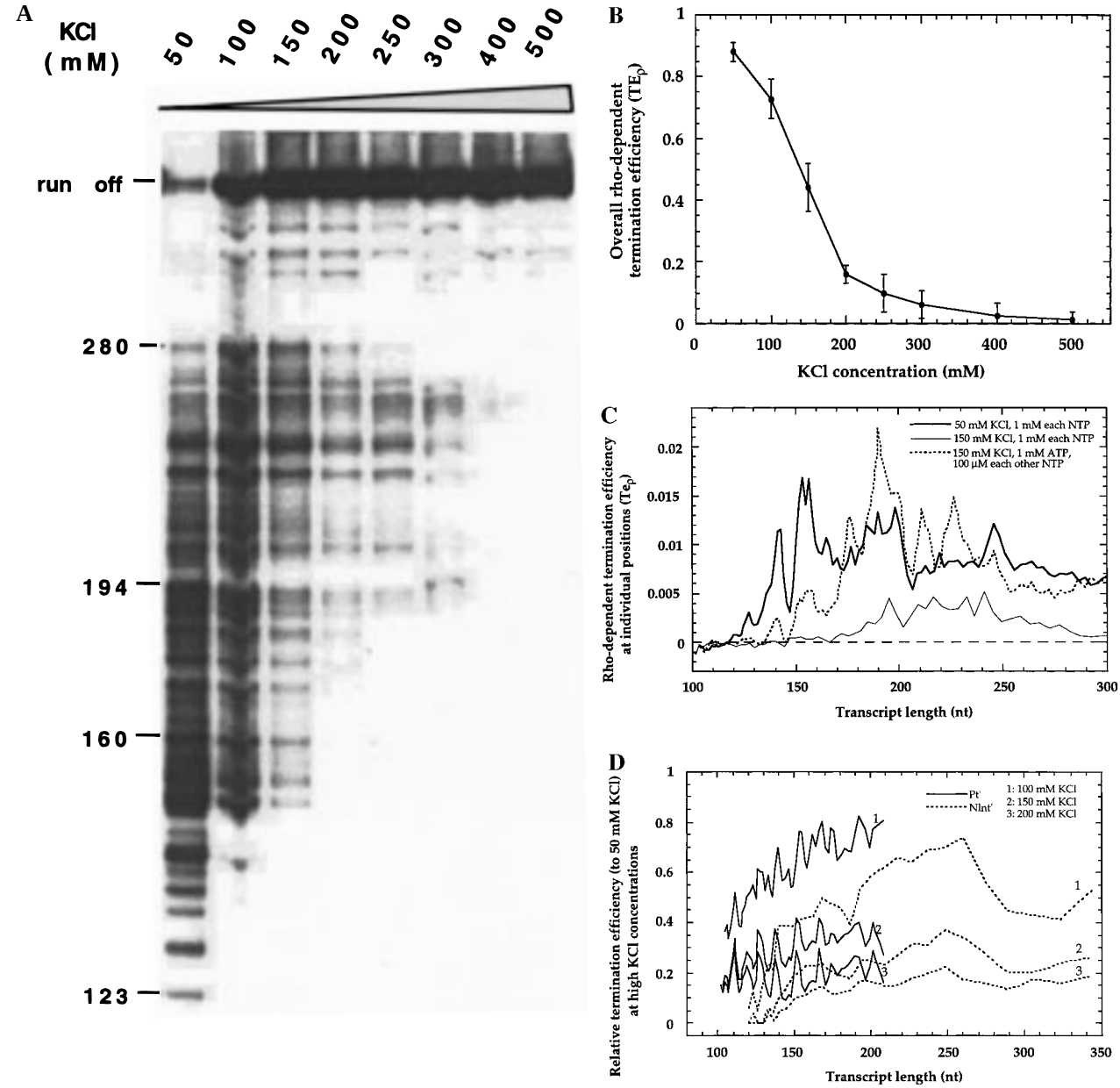

FIGURE 2: High monovalent salt concentrations shift the rho-dependent termination zone downstream while decreasing the termination efficiency at most positions, and these effects are only partially compensated by a slower rate of elongation. (A) Rho-dependent termination at different KCl concentrations. Transcription reactions were performed as described in Materials and Methods of ref *1*, in the presence of 5 nM NInt′ template, 5 nM RNA polymerase, 20 nM rho hexamer, and 1 mM concentrations of each NTP. Reactions contained 20 mM Tris-HCl (pH 7.9), 5 mM $MgCl_2$, 1 mM β-ME, and increasing concentrations of KCl. The KCl concentrations in lanes 1−8 were 50, 100, 150, 200, 250, 300, 400, and 500 mM, respectively. Transcript sizes were determined using RNA ladders run in parallel (not shown), and representative transcript lengths are marked. (B) Plot of TE_ρ as a function of KCl concentration in the reaction. Data from Figure 2A. Calculations of the TE_ρ parameter were made as described in Materials and Methods and Figure 3A of ref *1*. (C) Plots of rho-dependent termination efficiency for individual positions (Te_ρ) at different KCl and NTP concentrations as a function of transcript length. Some data are from Figure 2A. The dark solid line corresponds to the rho-dependent termination reaction under our standard reaction conditions (50 mM KCl, 5 mM $MgCl_2$, and 1 mM concentrations of each NTP). The faint solid line corresponds to the reaction in 150 mM KCl and 1 mM concentrations of each NTP, while the dotted line corresponds to the reaction in 150 mM KCl, 1 mM ATP, and 100 μM concentrations of each of the other NTPs. Calculations of the Te_ρ parameter were performed as described in Materials and Methods and Figure 3A of ref *1*. The broken horizontal line corresponds to 0 rho-dependent termination efficiency. (D) Plots of Te_ρ at higher KCl concentrations relative to Te_ρ at 50 mM KCl as a function of the template position. Some data are from Figure 2A. The dotted lines correspond to transcription on template NInt′, while the solid lines represent transcription on template Pt′. Relative (to standard reaction conditions; i.e., 50 mM KCl) values of Te_ρ were calculated for each template position. The curves numbered 1, 2, and 3 in each group are for 100, 150, and 200 mM KCl, respectively.

The fact that a decrease in transcript elongation rate does increase Te_ρ at corresponding sites in the downstream region suggests that kinetic competition does function at these sites in 150 mM KCl. Why then is a comparable competition not seen at the proximal sites of the RNA release pattern in 150 mM KCl? As shown in particular in the rho helicase studies of Walstrom et al. (*10*, *11*), rho action is sequential and can be divided into three distinct phases. These are (i) the loading of rho onto the transcript, accompanied by the RNA-dependent activation of the rho ATPase; (ii) translo-

cation of the rho hexamer 5′ → 3′ along the nascent RNA; and (iii) rho-dependent separation of the RNA−DNA hybrid. Since kinetic competition at distal sites argues that neither impairment of rho translocation nor impairment of rho-dependent separation of the RNA−DNA hybrid can be responsible for the reduction of the efficiency of rho-dependent termination at the proximal sites as a consequence of increased salt concentration, the only possibility remaining is the salt concentration dependent inhibition of the rho loading and/or of the ATPase activation events. In light of the demonstration (ref *1*) of a downstream shift of the termination zone due to the insertion of a defined hairpin structure into the RNA, these results suggest that the formation of increased secondary structure in the RNA at higher KCl concentrations (as demonstrated directly for this RNA transcript in ref *8*) may comparably increase the contour length of RNA that is required to form a functional rho loading site. This interpretation is consistent with the results presented in Figure 2D, in that rho-dependent termination at most downstream positions is more resistant to increased KCl concentrations, perhaps reflecting the increased transcript length available to form a functional rho loading site at these positions. These observations are not consistent with a dominant salt-dependent decrease in the processivity of translocation of rho along the transcript, since in this case one would expect to see a major decrease in relative termination efficiency with increased transcript length.

Figure 2D also shows that transcription complexes located between positions +110 and +210 on template Pt′ share a similar trend in the recovery of rho-dependent termination with positions +140 to +260 on the NInt′ template, even though, as a consequence of the insertion of a 42-bp element containing *nutL* into NInt′, and the replacement of the natural *trp t′* termination zone with plasmid DNA (114 nt) in Pt′, the local sequences in these regions on the two templates are completely different (Figure 1 of ref *1*). We showed previously that the termination patterns for these templates also share no similarity in these regions (see Figure 5A of the preceding paper). With the rho loading site representing the only common sequence located upstream of these regions on the two templates, we propose that the similar recovery trend at these regions on both templates must reflect a common rho loading event, and that the effects of increasing KCl concentration on the rho-dependent RNA release patterns are focused on the rho loading process (see also below).

However, the relative termination efficiency takes on an opposite trend starting at position +260 on template NInt′, which happens to be located about 80 nts away from the downstream limit of the rho loading site [position +174 as defined by Galloway and Platt (*12, 13*); see also Figure 1 of ref *1*]. The Pt′ and NInt′ templates share the same sequence over template regions +133 to +238 of Pt′ and +283 to +388 of NInt′, which are located at the downstream ends of both templates (see Figure 1, ref *1*). Yet we note that the upstream trend is continued over template positions +133 to +210 on Pt′, but not over template positions +283 to +320 on NInt′.

This result shows that the decrease in the relative termination efficiency with transcript length seen in the +260 to +320 region of the NInt′ template is not a general effect of the local sequence or of its location at the end of the template. Rather it may reflect some long-range effect on rho action due to the insertion of the 106 bps of natural *trp t′* terminator sequence. We suggest that rho-dependent termination at positions beyond ~80 nts downstream of the rho loading site requires translocation of rho along the nascent RNA. Thus the further downstream the transcription complexes are positioned, the more sensitive they are likely to be to high salt concentrations because the translocation of rho along the RNA transcript at higher salt concentrations is less processive, decreasing the probability of the arrival of the rho hexamer at downstream transcription complexes. Positions downstream of +210 on Pt′ and of +350 on NInt′ were not analyzed because their RNA products are located too close to the runoff transcript band on the gels to permit accurate analysis.

Thus plotting the relative termination efficiency as a function of template position on both the Pt′ and NInt′ templates in Figure 2D shows that (i) the decrease in effective rho-dependent termination at proximal template positions at the higher KCl concentrations reflects primarily decreased rho loading, rather than a salt concentration dependent decrease in the processivity of rho translocation along the transcript; (ii) the relief from the inhibitory effect of high salt with an increase in the transcript length is largely independent of local sequence; and (iii) that the opposite "polarity"-like effect beyond about position +260 on NInt′ is due neither to an unexplained transcript "end effect" nor to a local sequence effect, but rather is likely to reflect a long-range processivity effect related to rho function. We also conclude that increasing salt concentration has two major effects. These are (i) to effectively "shorten" the RNA transcript by increasing secondary structure within the rho loading site (perhaps because rho can effectively "step across" elements of looped-out secondary structure in translocating along the transcript), leading to a downstream shift of the position of the termination zone and thus to a relative increase in the effectiveness of rho-dependent termination at more distal template positions; and (ii) to a decrease in the processivity of rho translocation along the nascent RNA, leading eventually to a decrease in rho-dependent termination at still more distal template positions. These results are fully consistent with the results of Walstrom et al. (*8, 10, 11*) on the effects of increasing salt concentrations on the RNA−DNA helicase activity of rho in experiments using the same transcripts.

(ii) Effects of Increased $MgCl_2$ Concentration. We have also examined the effects of increasing the concentration of the Mg^{2+} cation on rho-dependent RNA release patterns for all the templates. Figure 3A shows the behavior of typical positions on the NInt′ template under different Mg^{2+} and substrate concentrations by plotting the rho-dependent termination efficiency at individual positions as a function of the transcript length under standard (5 mM; dark solid lines) and high (20 mM; faint solid lines) $MgCl_2$ concentrations. In Figure 3B we plot the relative rho-dependent termination efficiency at individual template positions in 10 mM Mg^{2+}, normalized to Te_ρ in 5 mM Mg^{2+} at the same template positions. The dotted line represents the relative release pattern for template Pt′, the dark solid line the relative release pattern for the Int′ template, and the faint solid line the relative release pattern for template NInt′. The results in both figures are quite comparable to those seen with increasing KCl concentrations. Again, both figures show

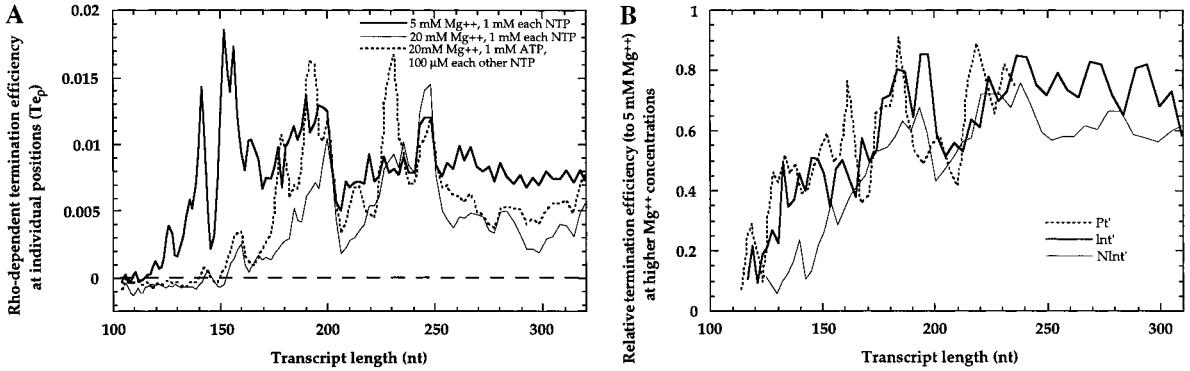

FIGURE 3: High Mg^{2+} concentrations shift the rho-dependent termination zone downstream while decreasing the termination efficiency at most positions, and these effects cannot be completely compensated by a slower elongation rate. Results shown are for transcription and rho-dependent termination on the NInt′ template. (A) Plots of rho-dependent termination efficiency for individual positions (Te_ρ) along the NInt′ template at different $MgCl_2$ and NTP concentrations as a function of transcript length. The dark solid line corresponds to the rho-dependent termination process under our standard reaction conditions (50 mM KCl, 5 mM $MgCl_2$ and 1 mM concentrations of each NTP). The faint solid line corresponds to rho-dependent termination in 20 mM $MgCl_2$, and 1 mM NTPs, while the dotted line corresponds to rho-dependent termination in 20 mM $MgCl_2$, 1 mM ATP, and 100 μM concentrations of each of the other NTPs. Transcription reactions were performed as described in Materials and Methods of ref *1*, using 5 nM DNA template, 5 nM RNA polymerase, and 20 nM rho hexamer. Each reaction contained 20 mM Tris-HCl (pH 7.9), 50 mM KCl, 1 mM β-ME, and 5 or 20 mM $MgCl_2$. Calculations of Te_ρ values were performed as described in Materials and Methods and Figure 3A of ref *1*. (B) Plots of relative Te_ρ values at 10 mM Mg^{2+} concentrations (relative to 5 mM Mg^{2+} concentrations) as a function of template position on all three templates. Each reaction contains 20 mM Tris (pH 7.9), 50 mM KCl, 1 mM β-ME, and 5 or 10 mM $MgCl_2$. The relative (to 5 mM Mg^{2+} conditions) values of Te_ρ were calculated for each template position. The dotted line plots the relative Te_ρ values measured with the Pt′ template, the dark solid line plots the values measured with the Int′ template, and the faint solid line plots those measured with the NInt′ template.

that increasing the concentration of Mg^{2+} decreases termination efficiency at all template positions, and that this decrease is most significant in the proximal portions of the *trp t′* terminator, resulting in an apparent downstream shift of the termination zone. For the same reasons described in connection with Figure 2C, we decreased the elongation rate of RNA polymerase by decreasing NTP concentrations. The dotted line of Figure 3A corresponds to the transcription reaction performed at 20 mM $MgCl_2$ under substrate concentration condition *3* (see above). Clearly a decreased elongation rate can increase the rho-dependent termination efficiency at only distal positions along the template, but cannot restore the proximal termination positions that were active in 5 mM $MgCl_2$.

To further confirm that the effects of higher Mg^{2+} concentrations on rho-dependent termination do not reflect an increase in the RNA polymerase elongation rate, we also measured the rate of elongation on the NInt′ template under different $MgCl_2$ concentrations. Results included in Table 1 show that an increase in $MgCl_2$ concentration from 5 to 20 mM *decreases* the rate of transcript elongation.

Thus it appears that both high K^+ and high Mg^{2+} concentrations shift the rho-dependent termination zone downstream and decrease rho-dependent termination efficiency, independent of any increase in the transcript elongation rate, and that kinetic competition exists at distal sites but not at proximal sites under these conditions. Thus the effects on proximal rho-dependent RNA release cannot be compensated by a slower elongation rate. These results again demonstrate the necessity for proper rho loading onto the transcript before kinetic competition with the transcription complex can be established.

DISCUSSION

Characterization of the Rho-Dependent Termination Process. In this study we have carried out a detailed functional study of the effect of kinetic competition and rho−RNA interactions on rho-dependent termination at the *trp t′* terminator. Our findings may be summarized as follows.

(i) Decreasing the rate of elongation of the transcript by limiting the concentration of the next required nucleotide can increase the heights of the individual peaks of the RNA release patterns without changing the overall shapes of the RNA release patterns. This shows that kinetic competition between the rates of rho and polymerase action can indeed control the efficiency of rho-dependent RNA release at a given template position, but only in a termination zone within which rho can act. In contrast, the template position of the upstream limit of rho-dependent termination cannot be shifted by kinetic competition.

(ii) The position of this upstream limit, and thus the position of the zone of opportunity for rho-dependent termination, depends on the synthesis of a length of RNA transcript sufficient to form an effective loading site for the rho hexamer. The total length of RNA that is required to form a functional rho loading site can be increased by introducing additional elements of RNA structure into the nascent transcript, either specifically by inserting a sequence that can form an RNA hairpin that can be looped out (*1*), or nonspecifically by increasing the concentrations of mono- or divalent cations as shown here. The result is a distal shift of the zone of opportunity for rho-dependent termination. The model we present in Figure 4 illustrates our interpretation of how RNA secondary structure within the rho loading site can shift the termination zone downstream.

(iii) At sufficiently high salt concentration conditions (e.g., >200 mM KCl), rho action is abolished altogether without affecting transcript elongation, presumably reflecting both increased formation of RNA secondary structure and decreased stability of the rho−RNA complex. The efficiency of rho-dependent termination decreases at intermediate salt concentrations, probably both because rho is unable to bind stably to the RNA to form a properly "articulated" loading complex and because the decreased binding affinity of rho

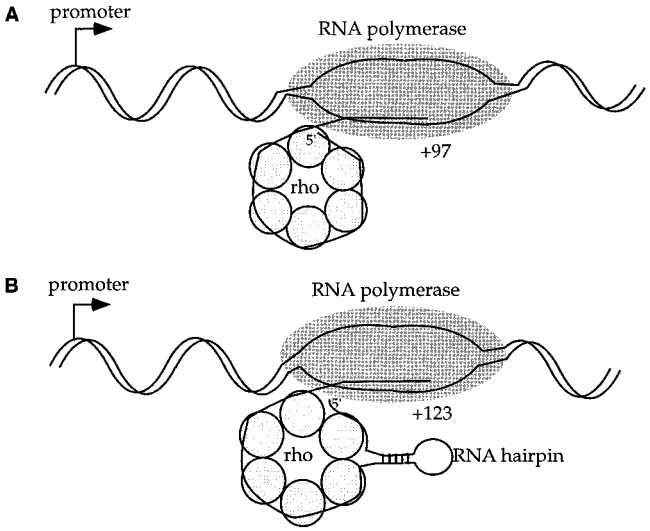

FIGURE 4: Model for the rho-loading event during rho-dependent transcription termination. (A) A rho hexamer loads onto the nascent RNA transcript and starts termination as soon as a stretch of unstructured RNA ~70−80 nt in length (see text) has been synthesized and extruded from the transcription complex to serve as a rho loading site. (B) Secondary structure elements (here an RNA hairpin containing ~15 nts) on the nascent transcript cannot bind to rho and therefore are effectively looped out. As a consequence a longer RNA transcript is required for rho loading and the zone of rho-dependent termination is shifted downstream.

for the nascent transcript decreases the processivity of translocation of rho along the RNA transcript (see also discussion of this point in ref *8*).

Rho Structure and the Interactions of Rho with RNA. Functional rho protein exists as a hexamer of subunits of identical amino acid residue sequence (*14*, *15*). These subunits are noncovalently joined in a hexagon (*16*−*19*). Each subunit carries binding sites for RNA and for ATP, and the six RNA binding sites are located around the periphery of the rho hexagon (*20*). The overall size of the RNA binding site of the rho hexamer (determined by footprinting with RNaseA) is ~70 nts for unstructured polynucleotides (*21*). Binding to RNA activates the RNA-dependent ATPase activity of rho (*22*−*25*), and all six subunit binding sites must be occupied by RNA to activate the rho ATPase beyond ~10% of its full specific activity (*26*).

These structural and enzymatic features of rho are compatible with the results presented in this study. Thus we have shown that a minimum of 97 nts of RNA must be synthesized to permit loading of the rho hexamer onto the nascent transcript in the presence of an actively synthesizing transcription elongation complex (*1*). A minimal RNA binding site size of ~70 nts for the rho hexamer alone is certainly compatible with this finding, suggesting that 20−30 nts at the 3′ end of the transcript are involved within the elongation complex and thus are not initially accessible to rho.

The fact that all six RNA binding sites of the rho hexamer must be occupied in order to turn on the RNA-dependent ATPase activity of rho to a significant level (*26*), coupled with the fact that this ATPase activity is essential for rho-dependent termination (*23*), also offers an explanation of how RNA secondary structure within the rho loading site could shift the proximal boundary of the zone of opportunity for rho-dependent termination downstream along the template, and why abolishing such secondary structure might shift the boundary back (*1*). Such a model is presented in Figure 4, and shows how the presence of a well-defined element of RNA secondary structure (such as the boxB RNA hairpin) could be "looped out" of the rho−RNA complex, resulting in a requirement for the synthesis of a longer transcript segment before the six RNA binding sites of the subunits of rho are all filled. Less defined elements of RNA secondary structure, including base stacking along the single-stranded RNA, which might be induced by elevated K^+ or Mg^{2+} concentrations, could also make regions of the nascent transcript less appropriate for rho binding (*27*) and thus support the requirement for an effectively longer rho loading site. Alternatively, a less effective rho−RNA complex could lead to diminished rho ATPase activation (*27*) and could also result in a diminished overall rho-dependent termination activity (see also ref *6*).

A Quantitative Model for Rho-Dependent Termination Efficiency. In this study we have identified several mechanistic components of rho function that work together to control the apparent overall efficiency of rho-dependent termination at a given template position ($Te_{\rho,\ observed}$). $Te_{\rho,\ observed}$ can be read from rho-dependent RNA release pattern plots such as Figures 2C and 3A of this paper, and Figure 5 of ref *1*. In the very "broad" *trp t′* terminator this parameter ranges from apparent (per template position) rho-dependent termination efficiencies of 0.03 down to efficiencies of 0.001 or less. In more homogeneous terminators, such as *λtR1*, this parameter can range up to 0.2 or higher at a given template position (see gels and figures in ref *28*). At saturating concentrations of NTPs and under fully processive rho activity conditions (i.e., at lower salt concentrations and perhaps physiologically as a consequence of macromolecular crowding) there is clearly a functional component reflecting the sequence of the template and the RNA at or near the putative 3′ end of the transcript. This parameter is measured and interpreted quantitatively elsewhere (A. Q. Zhu, M. O'Neill, and P. H. von Hippel, manuscript in preparation).

Under nonprocessive conditions (i.e., at higher salt or reduced NTP concentrations), $Te_{\rho,\ observed}$ is reduced by a processivity factor, *P*, which represents the fraction of the rho hexamers that bind initially to the rho loading site and actually reach the transcription complex. (As defined, *P* must be ≤ 1.0). In addition, $Te_{\rho,\ observed}$ contains a kinetic competition term $(\zeta k_{term})/(Kk_{elong} + \zeta k_{term})$, where k_{term} and k_{elong} correspond to the maximum rates of termination and elongation, respectively, and ζ and *K* represent condition-dependent factors that modulate the respective rates (both ζ and K must also be ≤ 1.0). These ζ and K parameters can be regulated either by changes in the concentrations of the NTP substrates (see Figures 1, 2C, and 3A of this paper) or by mutations in the polymerase or rho proteins themselves (see ref *3*). Thus the final value of the observed rho-dependent termination efficiency at a given template position can be written:

$$Te_{\rho,\ observed} = (Te_{\rho,\ sequence})(P)[(\zeta k_{term})/(Kk_{elong} + \zeta k_{term})] \quad (2)$$

where only the last term (in square brackets) is regulated by kinetic competition. In a subsequent paper (A. Q. Zhu, M.

O'Neill, and P. H. von Hippel, manuscript in preparation) we attempt to evaluate this kinetic competition term under processive conditions. Our results suggest that this parameter does indeed contribute only part of the total value of $Te_{\rho,\ observed}$, which is also heavily dependent on $Te_{\rho,\ sequence}$. However, the separation of rho-dependent termination efficiency (per position) into the various parameters that are summarized in eq 2 helps us to focus on what elements must be considered in attempting to interpret observed termination efficiency values ($Te_{\rho,\ observed}$) at defined template positions and under a variety of experimental conditions.

ACKNOWLEDGMENT

We are grateful to Dr. Terry Platt and his laboratory at the University of Rochester for the generous gift of plasmids pSP65t′ and pGEM1ΔMBt′, to Katherine Walstrom of this laboratory for providing rho protein, and to Marc Van Gilst and Feng Dong for helpful discussions.

REFERENCES

1. Zhu, A. Q., and von Hippel, P. H. (1998) *Biochemistry 37*, 11202−11214.
2. Capellos, C., and Bielski, B. H. J. (1972) in *Kinetic Systems: Mathematical description of chemical kinetics in solution*, Wiley-Interscience, New York.
3. Jin, D. J., Burgess, R. R., Richardson, J. P., and Gross, C. A. (1992) *Proc. Natl. Acad. Sci. U.S.A. 89*, 1453−1457.
4. Wilson, K. S., and von Hippel, P. H. (1994) *J. Mol. Biol. 244*, 36−51.
5. Rees, W. A., Weitzel, S. E., Das, A., and von Hippel, P. H. (1997) *J. Mol. Biol. 273*, 797−813.
6. Richardson, J. P., and Macy, M. R. (1981) *Biochemistry 20*, 1133−1139.
7. Draper, D. E. (1996) *Trends Biochem. Sci. 21*, 145−149.
8. Walstrom, K. M., Dozono, J. M., and von Hippel, P. H. (1998) *J. Mol. Biol. 279*, 713−726.
9. Chan, C. L., and Landick, R. (1997) *J. Mol. Biol. 268*, 37−53.
10. Walstrom, K. M., Dozono, J. M., Robic, S., and von Hippel, P. H. (1997) *Biochemistry 36*, 7980−7992.
11. Walstrom, K. M., Dozono, J. M., and von Hippel, P. H. (1997) *Biochemistry 36*, 7993−8004.
12. Galloway, J. L., and Platt, T. (1986) in *Regulation of Gene Expression*, 25 Years on Symposium of the Society for General Microbiology (Booth, I., and Higgins, C., Eds.) pp 155−178, Cambridge University Press, Cambridge, U.K.
13. Galloway, J. L., and Platt, T. (1988) *J. Biol. Chem. 263*, 1761−1767.
14. Finger, L. R., and Richardson, J. P. (1982) *J. Mol. Biol. 156*, 203−219.
15. Geiselmann, J., Yager, T. D., Gill, S. C., Calmettes, P., and von Hippel, P. H. (1992) *Biochemistry 31*, 111−120.
16. Geiselmann, J., Seifried, S. E., Yager, T. D., Liang, C., and von Hippel, P. H. (1992) *Biochemistry 31*, 121−132.
17. Seifried, S. E., Bjornson, K. P., and von Hippel, P. H. (1991) *J. Mol. Biol. 221*, 1139−1151.
18. Gogol, E. P., Seifried, S. E., and von Hippel, P. H. (1991) *J. Mol. Biol. 221*, 1127−1138.
19. Horiguchi, T., Miwa, Y., and Shigesada, H. (1997) *J. Mol. Biol. 269*, 514−528.
20. Geiselmann, J., Wang, Y., Seifried, S. E., and von Hippel, P. H. (1993) *Proc. Natl. Acad. Sci. U.S.A. 90*, 7754−7758.
21. Bear, D. G., Hicks, P. S., Escudero, K. W., Andrews, C. L., McSwiggen, J. A., and von Hippel, P. H. (1988) *J. Mol. Biol. 199*, 623−635.
22. Lowery-Goldhammer, C., and Richardson, J. P. (1974) *Proc. Natl. Acad. Sci. U.S.A. 71*, 2003−2007.
23. Howard, B., and de Crombrugghe, B. (1976) *J. Biol. Chem. 251*, 2520−2524.
24. Lowery, C., and Richardson, J. P. (1977) *J. Biol. Chem. 252*, 1375−1380.
25. Lowery, C., and Richardson, J. P. (1977) *J. Biol. Chem. 252*, 1381−1385.
26. Wang, Y. (1993) Ph.D. Thesis, University of Oregon.
27. Faus, I., and Richardson, J. P. (1989) *Biochemistry 28*, 3510−3517.
28. Morgan, W. D., Bear, D. G., and von Hippel, P. H. (1983) *J. Biol. Chem. 258*, 9553−9564.

BI972912S